A Survey of Energies in Materials Science

Frans Spaepen

Division of Engineering and Applied Sciences

Harvard University, Cambridge MA 02138, USA

Dedicated to J. David Embury on the occasion of his 65th birthday.

Abstract

A table is presented that compares energies that govern a variety of phenomena in materials science: thermal, structural and chemical energies; energies associated with the formation of vacancies, dislocations and interfaces; energies associated with the application of an external load, strain, magnetic field, or supersaturation. A simple argument, based on the polytetrahedral nature of the structure of liquids, is presented to explain why the configurational part of the entropy of melting for many elements is close to 1k.

1. Introduction

David Embury likes the big picture. In our many discussions over the years, which covered an amazing range of topics in materials science, we often found ourselves assessing a new or old problem by comparing its underlying energies. These conversations produced small diagrams, which I started collecting into an overall chart, which after a while turned into an interesting synthesis of much of materials science. I used the occasion of the Symposium in David's honor to turn this chart into a talk and into this paper. I will give some examples of its use, and I hope that it will inspire others to add comparisons and entries. Most of the data on the chart are for copper.

2. Energy unit

An upper limit for the energies to be considered for phenomena in materials science is the energy of the chemical bond. Energy changes that involve valence electrons are on the order of the Rydberg, the binding energy of the electron in the hydrogen atom:

$$Ry = \frac{me^4}{8\varepsilon_0^2 h^2} = 13.61 \ \ eV \tag{1}$$

where m is the mass of the electron, e the elementary charge, ε_0 the permittivity of the vacuum and h Planck's constant. The natural unit for the (logarithmic) scale for the energies per atom represented in Figure 1 is therefore the eV per atom.

3. Thermal energy and the temperature scale

In the classical equipartition regime, the amount of thermal energy per degree of freedom is 1/2 kT, where k is Boltzmann's constant and T the absolute temperature. For an atom in the condensed phase, there are six such degrees of freedom (three translational, three positional). The thermal energy per atom is therefore 3kT, which makes kT the natural temperature scale. The quantum mechanical correction of the thermal energy at low temperature can be estimated from the Debye model:

$$E_{thermal} = 3kT \ . \ 3\left(\frac{T}{\theta_D}\right)^3 \int_0^{\theta_D/T} \frac{u^3 du}{e^u - 1} \qquad (2)$$

where θ_D is the Debye temperature (Lewis & Randall, 1961). Figure 1 shows the temperature-dependence of the heat content of crystalline copper, for which θ_D=315 K (Ashcroft & Mermin, 1976). Above θ_D, the heat content is 3kT; below θ_D, the deviations due to the quantum effects are apparent.

4. Structural energies

The reference state for structural comparisons is crystalline, face-centered cubic, copper. The energy of metastable crystals varies greatly depending on the structure. Hexagonal-close packed (h.c.p.) copper has only slightly higher energy than f.c.c, since only its next-nearest neighbors are different. Since the h.c.p. structure can be created from the f.c.c. structure by introducing stacking faults between every other of a stack of close-packed planes, the energy of h.c.p. can be estimated as $\gamma_{SF} A_{(111)}/2 = 13$ meV, where $\gamma_{SF} = 0.073$ J/m^2 is the stacking fault energy, which can be determined from the separation of partial dislocations (Hirth & Lothe, 1968), and $A_{(111)} = 5.66$ Å^2 is the area per atom in the close-packed plane. Body-centered cubic (b.c.c.) copper, which can be stabilized, for example, in thin layers sandwiched between b.c.c. metals such as Nb (Kung, et al., 1997), has a higher energy: 39 meV (Tang, et al., 2002).

The liquid state has a considerably higher energy: the heat of melting of copper is $\Delta H_M = 135$ meV (Hultgren, et al., 1963). This corresponds to an entropy of melting of $\Delta S_M = 1.15$ k. Remarkably, its value is similar for most simple metals ("Richards' rule"). The Appendix gives a new argument for this long-standing observation, based on the polytetrahedral structure of simple liquids. As a result of this value, the melting

temperature of copper (T_M= 1356 K) lines up almost exactly with the heat of melting in Figure 1.

Because the specific heat of the liquid is greater than that of the crystal, the energy difference between liquid and crystal decreases with decreasing temperature. It drops, depending on the cooling rate, to about half the heat of fusion at the glass transition temperature (Kauzmann, 1948), and is therefore indicated as a range of values on Figure 1.

The heat of vaporization of f.c.c. copper at room temperature is ΔH_v= 3.50 eV (Hultgren, et al., 1963). It is a measure for the cohesive energy that can also be considered an upper limit for the energy scale.

5. Chemical energies

Formation of chemical bonds, especially between elements with a large difference in electronegativity, can cause large changes in energy, which often overwhelm all other effects ("Chemistry always wins" -- W.D. Nix, private communication). For example, the heat of formation of CuO is -1.63 eV (Weast, 1971). The absolute value is indicated on Figure 1. The chemical effects in metallic alloying can be much smaller. For

example, the heat of mixing of equiatomic Cu-Ag is 20 meV (Miedema, 1976); it leads to phase separation, but no change in crystal structure. The value for Cu-Au is -93 meV, it leads to the formation of ordered compounds, still based on the f.c.c. structure. The value for Cu-Zr is -446 meV, which is strongly negative. As a result, the Cu-Zr phase diagram contains numerous intermetallic compounds. If the formation of these compounds is kinetically suppressed, the reaction of pure crystalline Cu and Zr produces sufficient energy to allow formation of an amorphous Cu-Zr alloy in the solid state (Michaelsen, et al., 1997).

6. Vacancies

The introduction of an atom fraction, x, of vacancies, with a formation energy Q, into a lattice raises the energy per atom by xQ. Figure 1 shows the result for copper, for which Q=1.17 eV (Shewmon, 1963). An atom fraction x = 0.1 is an upper limit for the stability of the lattice. The energy associated with the highest equilibrium fraction of vacancies is $x^{eq}_{\max} Q$ = 0.05 meV, where the vacancy fraction corresponds to that at the melting point. For phase transformations, such as amorphization, to be vacancy-induced therefore requires non-equilibrium vacancy concentrations, introduced, e.g. by ion implantation. Even under these conditions, the fraction of vacancies necessary to cause

amorphization is so high (close to 10%) as to be unrealistic. Ion-induced amorphization, therefore occurs primarily by the direct displacement of the atoms (kinetic energy), rather than defect creation.

7. Dislocations

Introduction of dislocations, at a density, ρ, (dislocation length per unit volume) increases the energy per atom of the lattice by:

$$E_{disl} = \frac{\mu b^2}{4\pi} \ln\left(\frac{4}{b\sqrt{\rho}}\right) \Omega\rho \qquad (3)$$

where μ is the shear modulus, b the Burgers vector and Ω the atomic volume (Hirth and Lothe, 1968). The factor $\sqrt{\rho}$ in the expression for the line tension takes into account elastic screening at high dislocation densities. The results for Cu, with μ=76 GPa and b=2.56 Å, are shown in Figure 1 for values of ρ up to the areal atomic density, $\Omega^{-2/3} = 2 \times 10^{15}$ cm^{-2}. As for vacancies, unrealistically high dislocation densities are required to induce structural transformations. The amorphization induced by mechanical alloying, therefore, is not the result of the storage of mechanical energy, but of chemical mixing.

8. Surfaces and interfaces

The presence of a surface or interface of area A with energy γ per unit area increases the energy of a system of volume V by $\gamma A\Omega/V$ per atom. The ratio A/V has the dimension of 1/L, where L is a length that is similar to the linear dimensions of the system; its exact value depends on the dimensionality and shape of the system. The results for Cu, with γ=1.25 J/m^2, the average surface energy (Cammarata, 1994), for L down to the atomic size are shown in Figure 1. Size-induced structural transformations become possible for clusters or grains on the order of 1 nm. For this comparison, γ should be taken as the *difference* between the surface energies of the two phases, and hence it has a smaller value than that used for the plot. An example is the 13-atom icosahedral cluster, typical of the polytetrahedral packing in a liquid, which has a 17% lower energy than the cuboctahedral one (the nearest-neighbor shell in f.c.c.) (Hoare & Pal, 1971).

9. External load

The work per atom required to add matter to a system at a facet with normal **n** (with vector components n_i)in the presence of an external stress $\boldsymbol{\sigma}$ (with tensor components σ_{ij}) is $n_i\sigma_{ij}n_j\,\Omega$ (Herring, 1950). Figure 1 shows the results for the hydrostatic case. For comparison to structural transformations, Ω should be taken as the

difference between the atomic volumes, in which case the scale drops by 1-2 orders of magnitude. It is apparent that large hydrostatic stresses (GPa) can indeed effect structural transformations.

Comparison with the scale for surfaces and interfaces reveals that particles with a diameter on the order of 10 nm have an internal pressure on the order of 100 MPa. Indeed, γ/L can be considered a Laplace pressure. It should be kept in mind, however, that for a solid particle, the pressure is f/L, where f is the surface *stress*, which is a tensor, distinct from the surface energy (Cammarata, 1994); its value can even be negative.

10. Elastic strain

The energy per atom associated with a uniaxial strain ε is

$$E_{strain} = \frac{1}{2} E \varepsilon^2 \Omega \qquad (4)$$

where E is Young's modulus. The plot in Figure 1 shows its value for copper, with E=198 GPa. For strains greater than a few percent these values are overestimates, since non-linear elastic effects have not been incorporated. The upper limit corresponds to the strain at the ultimate tensile strength (Dieter, 1961):

$$\varepsilon_{th} = \sqrt{\frac{\gamma}{Eb}} \tag{5}$$

which, for copper is 13%, which in turn corresponds to a stress of 26 GPa. Comparison with the previous entry makes it clear that the elastic strain contribution of the applied stress to the chemical potential (i.e., to the Helmholtz free energy) is considerably smaller than the volume work of the previous section.

The competition between strain energy and interfacial energy leads to the existence of a critical thickness, below which a strained epitaxial layer that forms a coherent interface with a substrate is stable. Figure 1 shows that a for layer strains on the order a few percent, the corresponding critical thickness is on the order of a nm, whereby the value of γ is that of the interface formed by the coherency dislocations (which is lower than the surface energy).

11. Magnetic energy

The energy density in a magnetic field B is

$$E_{mag} = \frac{1}{2}\frac{B^2}{\mu} \tag{6}$$

where μ is the magnetic permeability. Figure 1 shows the quantity $E_{mag}\Omega$, in which, to an excellent approximation for copper, $\mu=\mu_0= 4\pi\ 10^{-7}\ TmA^{-1}$, the permeability of vacuum. In a non-magnetic material like copper magnetic effects are unimportant: coupling is difficult (e.g., by eddy currents), and very large fields are required to compete with other contributions.

For ferromagnetic materials the effect is much stronger. The energy of magnetization of iron, obtained by integrating the magnetic contribution to the specific heat between 500 and 1500 K, using a straight line as a base line, is 53 meV (marked as "Fe" on Figure 1) (Braun, et al., 1965). Since this value is similar to the heats of structural transformation, it is not surprising that in these materials magnetic contributions may affect phase transitions. For example, the driving force for nucleation of (ferromagnetic) crystals from undercooled Co-Pd melts has an identifiable magnetic contribution (Holland-Moritz & Spaepen, 2004). The Curie temperature for iron is T_C=1039 K; the energy kT_C is similar to the energy of magnetization.

12. Supersaturation

The difference in chemical potential of an ideal gas at pressure p and temperature T is:

$$\mu = \mu_0 + RT \ln\left(\frac{p}{p_0}\right) \tag{7}$$

where μ_0 is the chemical potential of a reference state at T and p_0. If the vapor pressure of a material is Δp above the equilibrium pressure p_0, the corresponding increase in chemical potential is

$$\Delta\mu = RT \ln\left(1 + \frac{\Delta p}{p_0}\right) \tag{8}$$

This quantity is plotted as a function of $\Delta p/p_0$ in Figure 1, for $T=T_M$. The listed values for the supersaturations are easily reached, for example by raising the temperature of Knudsen cell that produces Cu vapor. The ratio of the equilibrium vapor pressure p at a temperature T to that at temperature T_0 can be estimated from:

$$\frac{p}{p_0} = \exp\left(\frac{\Delta H_v}{R}\left(\frac{1}{T_0} - \frac{1}{T}\right)\right) \tag{9}$$

where ΔH_v is the heat of vaporization mentioned above. Therefore, for a copper source at T_M = 1356 K, the supersaturation exceeds 10^3 for a sample at any temperature below 1100 K. Evaporation, and other means of physical and chemical deposition, are therefore powerful methods for producing metastable phases, such as amorphous materials, and microstructures with high energies, such as nm-scale samples or strained epitaxial layers.

A comparison of the supersaturation entries with the interfacial energies immediately shows the Gibbs-Thompson effect. For example, the vapor pressure in equilibrium with a 10 nm particle is 10% greater than the equilibrium pressure for an infinite system. Similarly, a 10% enhancement of the solubility into the matrix of the elements in a precipitate is expected for 1-10 nm particles, depending on the value of the interfacial energy.

13. Extension to other materials

The data used to construct Figure 1 are almost all for copper. The Figure can be extended to other f.c.c. metals because many of their properties, such as stiffnesses, defect energies, surface energies, etc. scale with the melting point, T_M. This is because the liquid state has a well-defined structure, just like f.c.c., and the energy difference between them scales with the bond energy or the cohesive energy, ε. Since the stiffness is approximately equal to ε/b^3 and the atomic size varies little, the stiffness also scales roughly with the cohesive energy. The formation energies of defects that create broken bonds, such as vacancies or surfaces obviously scale with ε. As a result, it is reasonable to normalize the energy scale of Figure 1 by kT_M to extend it to other f.c.c. metals as well.

Acknowledgements

Many of the discussions with David Embury that led to the overview presented here were held during the meetings of the Summer Research Group at the Center for Materials Science at Los Alamos National Laboratory, and during the meetings at LANL of the investigators of the program on ultra-high strength materials, sponsored by the US Department of Energy, Office of Science, Basic Energy Sciences.

References

Ashcroft, N.W., and Mermin, N.D., 1976, *Solid State Physics* (Holt, Rinehart and Winston), p.461.

Bernal, J.D., 1964, *Proc. Roy. Soc. London A - Math. Phys. Sci.* **280**, 299.

Braun, M., Kohlhaas, R., and Vollmer, O., 1965, *Z. Angew. Phys.* **25**, 365.

Cammarata, R.C., 1994, *Prog. Surf. Sci.* **46**, 1.

Dieter, G.E., 1961, *Mechanical Metallurgy* (Mc Graw-Hill), p.193.

Faber, T.E., 1972, *Introduction to the Theory of Liquid Metals* (Cambridge), pp. 74-109.

Finney, J.L., 1970, *Proc. Roy. Soc. London A - Math. Phys. Sci.* **319**, 479.

Frank, F.C., 1952, *Proc. Roy. Soc. London A - Math. Phys. Sci.* **215**, 43.

Granato, A.V., 1994, *J. Phys. Chem. Solids* **55**, 931.

Herring, C., 1950, *J. Appl. Phys.* **21**, 437.

Hirth, J.P, and Lothe, J., 1968, *Theory of Dislocations* (McGraw-Hill), p. 764.

Hoare, M.R., and Pal, P., 1971, *Adv. Phys.* **20**, 161.

Holland-Moritz, D., and Spaepen, F., 2004, *Phil. Mag.* **84**, 957.

Hultgren, R., Orr, R.L., Anderson, P.D., and Kelley, K.K., 1963, *Selected Values of Thermodynamic Properties of Metals and Alloys* (Wiley), p.92.

Kauzmann, W., 1948, *Chem. Rev.* **43**, 219.

Kung, H., Lu, Y.C., Griffin Jr., A.J., Nastasi, M., Mitchell, T.E., and Embury, J.D., 1997, *Appl. Phys. Lett.* **71**, 2103.

Lennard-Jones, J.E., and Devonshire, A.F., 1939, *Proc. Roy. Soc. A* **169**, 317.

Lewis, G.N., and Randall, M., 1961, *Thermodynamics* (McGraww-Hill), p. 659.

Michaelsen, C., Barmak, K., and Weihs, T.P,, 1997, *J. Phys. D.: Appl. Phys.* **30**, 3167.

Miedema, A.R., 1976, *Philips Tech. Rev.* **36**, 217.

Nabarro, F.R.N., 1967, *Theory of Crystal Dislocations* (Oxford).

Nelson, D.R., and Spaepen, F., 1989, *Solid State Physics* **42**, 1.

Seeger, A., 2001, *Z. Metallk.* **92**, 632.

Shewmon, P.G., 1963, *Diffusion in Solids* (McGraw-Hill), p.74.

Spaepen, F., and Meyer, R.B., 1976, *Scripta metall.* **10**, 257.

Tang, Z., Hasegawa, M., Nagai, Y., and Saito, M., 2002, *Phys. Rev. B.* **65**, 195108.

Weast, R.C., 1971, *Handbook of Chemistry and Physics* (CRC), p. D45.

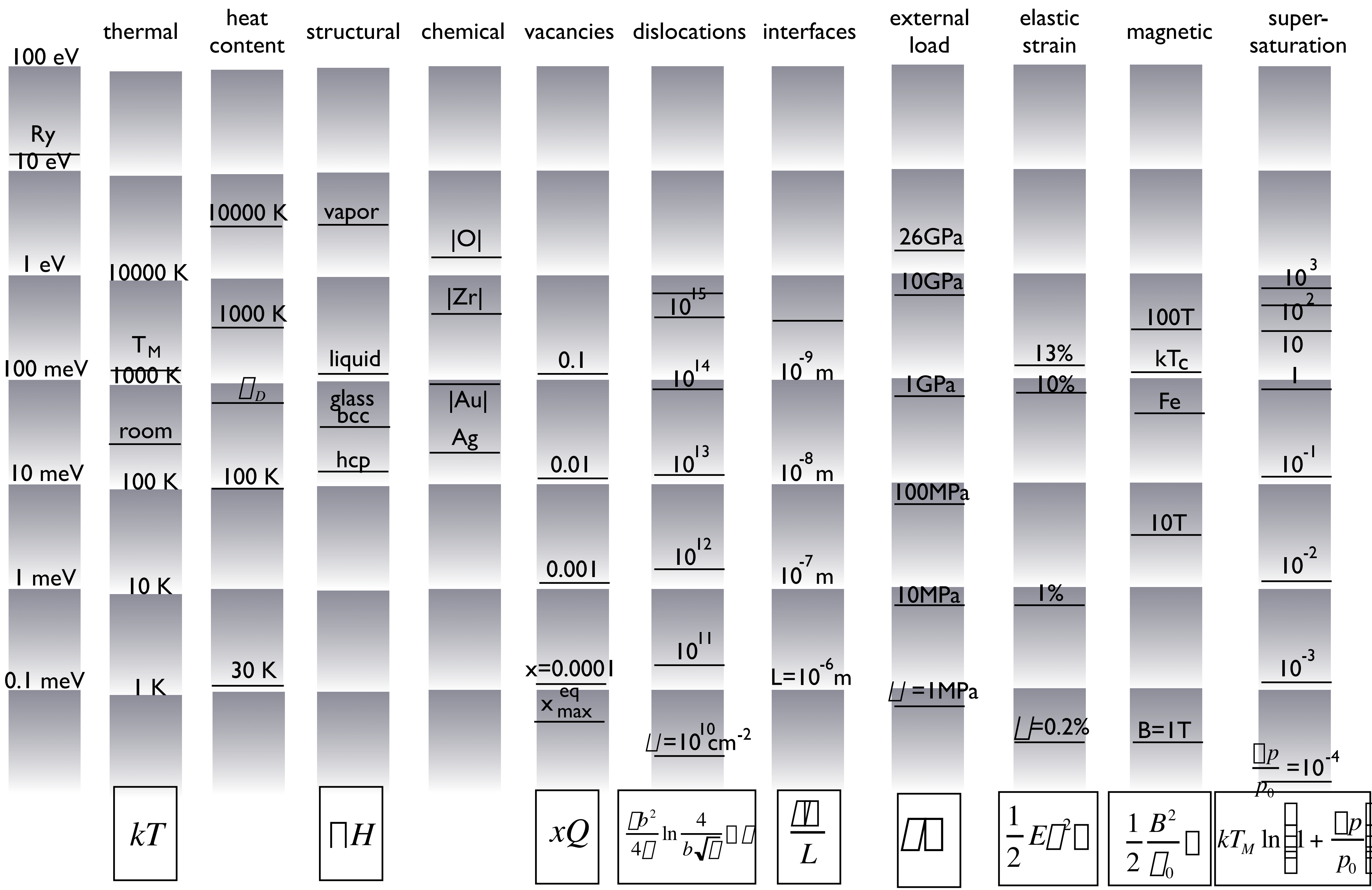

100 eV
Ry
10 eV
1 eV
100 meV
10 meV
1 meV
0.1 meV
thermal
10000 K
T_M
1000 K
room
100 K
10 K
1 K
kT
heat content
10000 K
1000 K
100 K
30 K
structural
vapor
liquid
glass
bcc
hcp
chemical
|O|
|Zr|
|Au|
Ag
vacancies
0.1
0.01
0.001
x=0.0001
x^{eq}_{max}
xQ
dislocations
10^{15}
10^{14}
10^{13}
10^{12}
10^{11}
$=10^{10}$ cm^{-2}
interfaces
10^{-9} m
10^{-8} m
10^{-7} m
L=10^{-6} m
L
external load
26GPa
10GPa
1GPa
100MPa
10MPa
=1MPa
elastic strain
13%
10%
1%
=0.2%
magnetic
100T
kT_c
Fe
10T
B=1T
super-saturation
10^3
10^2
10
1
10^{-1}
10^{-2}
10^{-3}
$=10^{-4}$

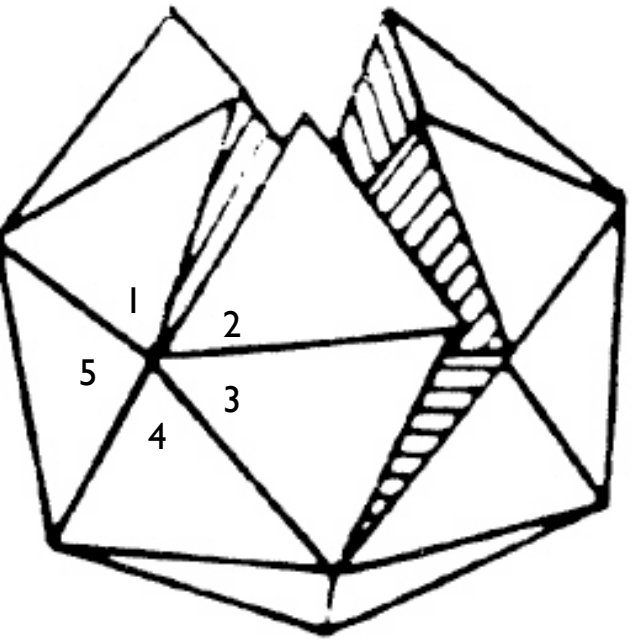

(a)

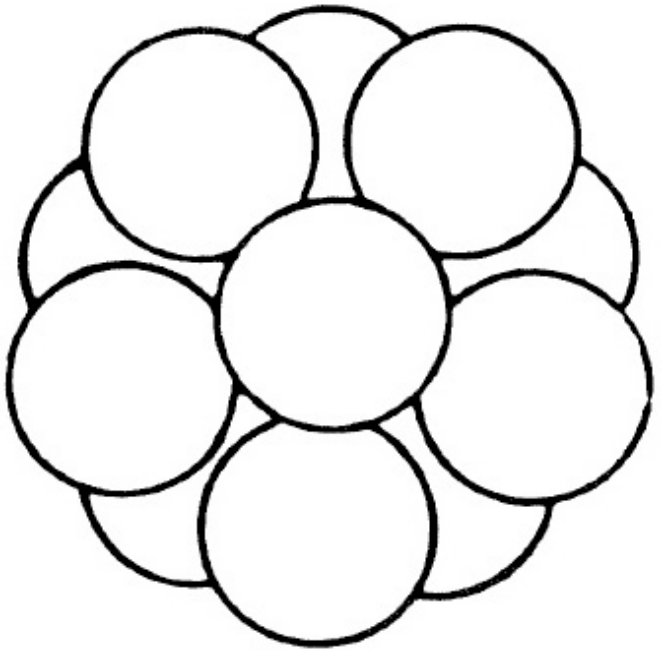

(b)

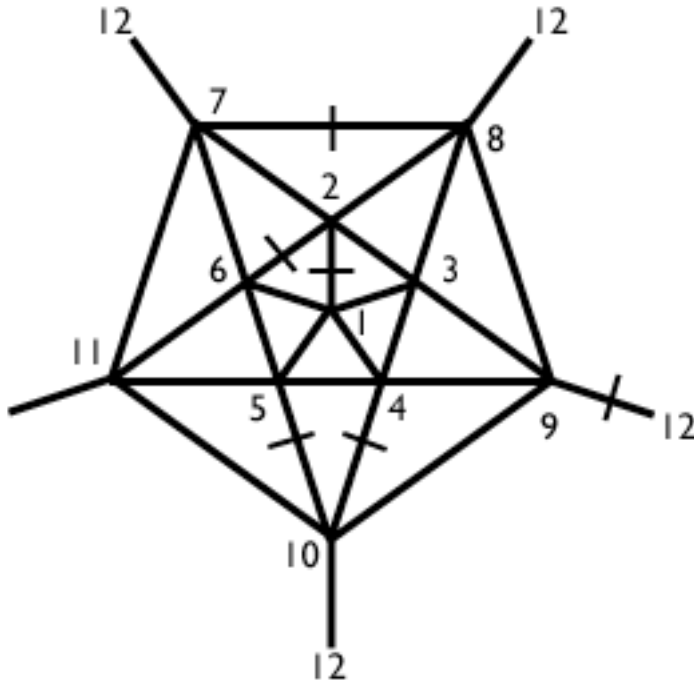

(c)

Figure Captions

Figure 1: Comparative table of energies used in materials science. Unless otherwise indicated, all physical quantities are for copper, with crystalline face-centered-cubic copper as the reference state.

Figure A1: (a) Packing of 20 regular tetrahedra around a common vertex, showing the gaps that must occur. (b) Icosahedral cluster of 12 hard spheres around a central one showing the gaps between the spheres. (c) Topology of the surface of an icosahedron. The six short lines indicate one configuration of possible gaps.

Appendix: Estimate of the Entropy of Melting of Simple Liquids Based on their Polytetrahedral Structure.

The entropy of melting of many elements is remarkably similar, around 1.2 k (Faber, 1972). Of this, about 0.2 k is an increase in the vibrational entropy that results from the lower density, and hence the lower vibrational frequency, in the liquid (Spaepen & Meyer, 1976). The remaining 1 k is the result of the increase in configurational entropy.

Many models of the liquid structure are based on the introduction of large number of defects into a crystalline lattice. Planar and line defects are too spatially correlated, in three dimensions, to produce sufficient entropy (Faber, 1972; Nabarro, 1967). The maximum entropy achievable with single point defects is kln(2)=0.69 k, at the unrealistic concentration of 0.5. The point defect entropy can be formally raised by considering Frenkel pairs (Lennard-Jones & Devonshire, 1939) or interstitialcy pairs (Granato, 1994). Nevertheless, the defect concentrations remain unrealistically large and, most importantly, these models require the formal persistence of translational and point symmetries of the crystals even when the liquid structure is supposedly reached.

In the opposite approach, the liquid is created by the densification of a gas and by accounting for the increasing degree of correlation between the atomic positions (Faber, 1972; Seeger, 2001). This approach provides satisfactory calculations of the liquid entropy, but does not give simple insight into the configurational degeneracy of the densest, i.e. liquid, structures.

The closest we have come to a one-word characterization of the liquid structure is "polytetrahedral" (Nelson and Spaepen, 1989) Alternatively, one could say that the liquid structure arises form maximizing the *local* density, in contrast with the close-packed crystals (f.c.c., h.c.p), in which the *overall* density is maximized. The densest local configuration that can be created with hard spheres is four of them at the vertices of a tetrahedron. Since the dihedral angle (i.e., the angle between adjacent faces) of a tetrahedron is $\cos^{-1}(1/3)= 70.53^0$, five tetrahedra can be packed around a common edge; they leave a gap of 7.36^0. This is illustrated by the tetrahedra numbered 1-5 in Figure A1(a).

The five-fold symmetry created by the local dense packing is inconsistent with the rotations allowed in periodic crystals (2-, 3-, 4-, or 6-fold). These five-fold rings are indeed ubiquitous in the dense random packing of hard spheres, the first successful structural model of the liquid (Bernal, 1964; Finney, 1970). Twenty tetrahedra can be

packed around a common vertex to form an icosahedron, which Frank (1952) proposed as the distinguishing structural characteristic of the liquid.. Since the edges of an icosahedron are 11% longer than the center-to-vertex distance, 12 hard spheres packed icosahedrally around a central one do not touch, as illustrated by Figure A1(b). Figure A1(a) illustrates the same in a different way: as regular tetrahedra are packed into an icosahedron, a number of gaps must be left. Since these gaps can be placed in a number of equivalent positions with little or no change in the energy of the cluster, this high configurational degeneracy provides a simple qualitative explanation of the fluidity of liquids.

The configurational degeneracy can be estimated by considering the topology of the icosahedron, as illustrated in Figure A1(c). An icosahedron has 12 vertices, 20 faces and 30 edges. The edges form 12 rings of five (for example: 2-3-4-5-6, 7-6-1-3-8 or 12-7- 2-3-9 in the Figure). Each of these rings must have (at least) one gap, for the geometric reasons given above. Each gap is shared by two rings. For example, the gap between vertices 2 and 6 is shared ring 2-3-4-5-6 and ring 8-2-6-11-12. The minimum number of gaps on the icosahedron is therefore six. The number of ways six gaps can be distributed over 30 edges, so that each ring has one gap can be estimated as:

$$W = 5\left(\frac{1}{5}\right)\left(\frac{4}{5}\right)^4 \frac{30!}{6!\ 24!} \qquad \text{(A1)}$$

The factorial part arises from the permutations of indistinguishable entities; the fractional factors in front limit the permutations to those that have only one gap per ring. The corresponding entropy, per atom in the 13-atom cluster, is:

$$S = \frac{1}{13} k \ln W = 0.95k \qquad \text{(A2)}$$

That this value is so close to 1k is somewhat fortuitous, given that the calculation is for a single, isolated cluster and that a number of approximations have been made. Nevertheless, the calculation illustrates that the configurational degeneracy is sufficiently high to provide the necessary entropy, since relaxation of the requirement of a single gap would provide additional configurations. On the other hand, energetic considerations tend to favor the formation of optimal nearest-neighbor distances, and hence the formation of single gaps.